Multifrequency High-Field Electron Paramagnetic Resonance Characterization of the Peroxyl Radical Location in Horse Heart Myoglobin Oxidized by H_2O_2

Tatyana A. Konovalova,[†] Lowell D. Kispert,*[,†] Johan van Tol,[‡] and Louis-Claude Brunel[‡]

Department of Chemistry, Box 870336, University of Alabama, Tuscaloosa, Alabama 35487, and Center for Interdisciplinary Magnetic Resonance, National High Magnetic Field Laboratory, Florida State University, Tallahassee, Florida 32310

Received: December 31, 2003; In Final Form: May 3, 2004

The peroxyl radical location in horse heart myoglobin (Mb) oxidized with H_2O_2 was examined by 9−287 GHz electron paramagnetic resonance (EPR) spectroscopy along with the radicals formed upon oxidation of tyrosine (Tyr), tryptophan (Trp), and histidine (His) individual amino acids. X-ray crystallography of the horse heart Mb has revealed that Tyr103, Tyr146, Trp14, and His64 residues are in the vicinity of the Mb heme group and thus could be implicated in Mb oxidation. The 9 GHz axial EPR signal of the Mb peroxyl radical ($g_{||} = 2.040 \pm 0.003$ and $g_{\perp} = 2.001 \pm 0.001$) is nearly identical with those of the radicals produced by irradiation of the individual amino acids in the presence of H_2O_2 (77 K). The 95−287 GHz measurements were sufficient to resolve the individual **g** tensor components of the Mb, Tyr, Trp, and His peroxyl radicals which cannot be distinguished at 9−35 GHz. The high-field EPR spectra of the Mb peroxyl radical were simulated using a Hamiltonian that describes the exchange and dipolar interaction between an oxoferryl iron and a protein radical. The exchange-coupled oxoferryl−protein radical pair could be best fitted with *g* values of $g_X = 2.0356$, $g_Y = 2.0083$, and $g_Z = 2.0024$ for the radical, a dipolar coupling corresponding to a distance of 8.3 Å between the radical and the oxoferryl iron, and an exchange coupling (*J*) of 0.476 GHz. The determined **g** tensor and the distance related to the Tyr residue at position 146. Tyr146 is assumed to be the most likely candidate for the peroxyl radical location in oxidized Mb.

1. Introduction

Increasing interest in the identification of the radical species formed in the reactions of heme proteins with hydroperoxides relevant in biological systems has been stimulated by the importance of these reactions in elucidating the origin of the lipid peroxidation[1] and the structural perturbations of proteins.[2] A catalytic site of myoglobin (Mb) consists of the iron−protoporphyrin IX group, heme, that provides hydrogen peroxide-dependent oxidation of the protein.[3] Because of the potential role of oxidized myoglobin as a mediator of myocardial reperfusion injury,[4] the nature of the oxidizing species and their location in the protein are of great importance. When Mb reductively cleaves H_2O_2 via a two electron process, these two electrons come from two separate sites: one from the heme iron, leading to the formation of an oxoferryl species (Fe^{4+}═O), and one from the protein, resulting in a transient-protein (globin)-centered free radical:[5]

$$\text{Mb heme } (Fe^{2+}) + HOOH \rightarrow Mb^{\bullet} \text{ heme } (Fe^{4+}{=}O) + H_2O$$

The long-lived Fe^{4+}═O species has been detected by optical absorption at ∼545 nm[6] and the protein radical by electron paramagnetic resonance (EPR) spectroscopy.[7,8] The transient protein radical most likely reacts rapidly with molecular oxygen to form peroxyl radicals or oxidizes external substrates.[9] Using molecular oxygen enriched with ^{17}O, Mason et al. have demonstrated that the radical observed in the reaction of Mb with H_2O_2 is a peroxyl radical.[10]

CHART 1: Heme Group of Horse Heart Myoglobin with Tyr103, Tyr146, His64, and Trp14 Amino Acid Residues (Resolution, 1.7 Å)

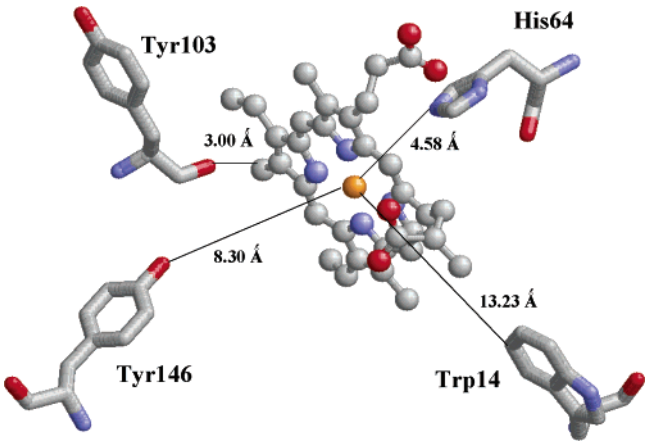

The location of the peroxyl radical in oxidized myoglobin has been discussed over the years. Several amino acid residues have been considered as possible sites of the protein radical formation. The saturation properties of the EPR signal of the Mb protein radical indicated that the radical is initially located on a phenylalamine or histidine and then is rapidly transferred to a tyrosine.[11] It was suggested that histidine may either act as a mediator in the transfer of an unpaired electron to the tyrosine residues or may participate directly in the oxidation process.[12] On the basis of the results of the EPR spin-trapping technique,

* To whom correspondence should be addressed. E-mail: Lkispert@bama.ua.edu. Phone: (205) 348 7134.
[†] University of Alabama.
[‡] Florida State University.

10.1021/jp0313425 CCC: $27.50
Published on Web 07/03/2004

the radical has been proposed to be a tyrosine (Tyr)-based radical.[13,14] On the other hand, site-directed mutagenesis studies have demonstrated that none of the tyrosine residues are essential for protein radical formation.[15] Mutagenesis of Mb implicated a tryptophan (Trp) residue that reacts with oxygen to give the peroxyl radical.[16] The radical centered on C3 of the indole ring of a tryptophan has been assigned as an initial radical.[17] Both mutagenesis and spin-trapping techniques have shown that radicals can be located on Trp14 or Tyr103 residues.[9] The Trp peroxyl and Tyr phenoxyl radicals have been identified in the reaction of horse heart and human Mb with H_2O_2.[18] The Tyr103 (at pH 7) and His64 (at pH 5) were identified as possible sites of Mb oxidation from analysis of the Mb−MNP spin adduct by electrospray mass spectroscopy.[19]

In this work, we studied the location of the peroxyl radical in horse heart Mb treated with H_2O_2 by the use of multifrequency EPR spectroscopy. Signals with unresolved *g* anisotropy, inherent in protein-based radicals at conventional fields (0.3 T, 9 GHz), can be resolved at higher frequencies. Further, the multifrequency characterization results in separation of the effects due to the *g* values from those due to hyperfine interactions. High-field EPR (HF-EPR) permits precise determination of the *g* values of biological radicals, provides parameters for accurate simulation of the EPR spectra, and allows determination of detailed information about the radicals themselves and their environment.[20−27]

The EPR parameters of the Mb radical were compared to those of the radicals formed by oxidation of the individual amino acids, namely, Tyr, Trp, and His. The particular amino acids were chosen because, according to the crystal structure of horse heart myoglobin at 1.7 Å resolution, there are Tyr103, Tyr146, Trp14, and His64 residues in the vicinity of the heme group (Chart 1).[28] Tyr103, which is closest to the heme,[29] could be the first residue to be oxidized. However, the unpaired spin moves rapidly between multiple sites in the protein, and other residues cannot be excluded in myoglobin oxidation.

2. Experimental Section

Chemicals. Myoglobin (horse heart) was purchased from Sigma and used without further purification. Potassium phosphate buffer (pH 7.0 ± 0.01 at 25 °C) was obtained from Fisher. Tyrosine (99%), tryptophan (99%), and histidine (99%) amino acids and aqueous hydrogen peroxide (30%) were all obtained from Aldrich.

Sample Preparation. The myoglobin solution in potassium phosphate buffer ($(3-5) \times 10^{-3}$ M) was mixed with equimolar hydrogen peroxide in the EPR tube and immediately frozen in liquid nitrogen. The tyrosine, tryptophan, and histidine solutions in potassium phosphate buffer (2.5×10^{-3} M) were treated with excess H_2O_2 to give a molar ratio of 1:1.5. The reaction was initiated by irradiation of the amino acid/H_2O_2 mixture with a Xe/Hg lamp (200 W) at 77 K.

EPR Measurements. X-band (9 GHz) EPR measurements were carried out with a Bruker ESP 300E EPR spectrometer. The magnetic field was measured with a Bruker EPR 023M gaussmeter, and the microwave frequency was measured with a model HP 5352B microwave frequency counter.

The 95−287 GHz measurements were performed at the high-field EPR facility of the National High Magnetic Field Laboratory (Tallahassee, FL). The spectrometer used was similar to that described by Mueller et al.[30] The fundamental microwave frequencies of 95 ± 3 and 110 ± 3 were generated by two Gunn oscillators, while higher harmonics of these were produced with a frequency multiplier. An EIP 578 frequency counter measured and locked the fundamental frequency. The 15 T Oxford Instruments superconducting magnet was typically swept at a rate in the range 0.5−6 mT/s. A modulation coil around the sample space produced 1−5 mT of field modulation at 8

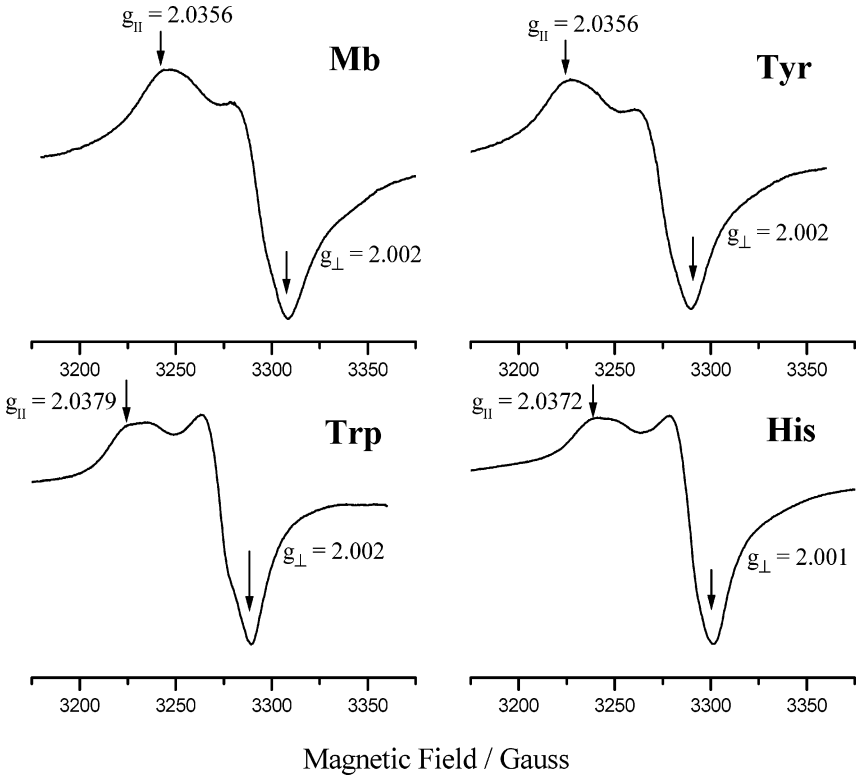

Figure 1. X-band EPR spectra (77 K) of peroxyl radicals generated by mixing solutions of Mb (5 mM) and H_2O_2 (5 mM) in phosphate buffer or by 300 nm irradiation of frozen (77 K) Tyr, Trp, and His solutions mixed with H_2O_2. Modulation amplitude, 4 G; modulation frequency, 100 kHz; microwave power, 2 mW.

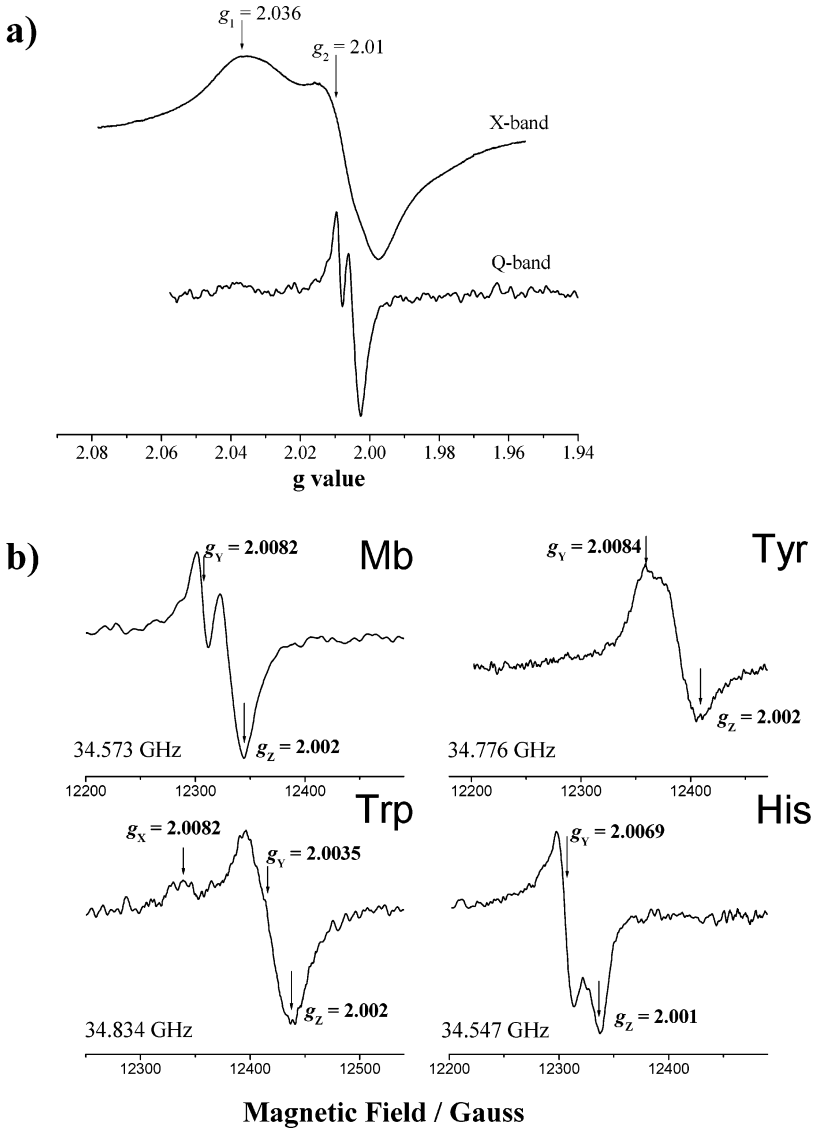

Figure 2. (a) EPR spectra of the Mb radical measured at 9.1 and 34.6 GHz at 77 K. (b) Q-band EPR spectra of the Mb, Tyr, Trp, and His radicals measured at 77 K using a modulation amplitude of 4 G and a microwave power attenuation of 24−30 dB.

kHz. As the spectrometer was operated in a single-pass transmission mode without a resonator, similarly sized samples could be measured at all frequencies. The samples were contained in a sealed 4 mm quartz EPR tube and placed in an Oxford Instruments CF 1200 continuous flow cryostat. A liquid-helium-cooled hot-electron InSb bolometer (QMC Instruments, U.K.) served as the (sub)millimeter-wave detector.

3. Results and Discussion

The Mb radical was produced by addition of hydrogen peroxide to the myoglobin solution in phosphate buffer (pH 7). Formation of the Tyr, Trp, and His radicals was initiated by 300 nm irradiation of the amino acid samples in the presence of H_2O_2 at 77 K. The resultant 9 GHz powder EPR spectra (77 K) exhibited signals with essentially identical principal values of the axial **g** tensor ($g_{||} = 2.040 \pm 0.003$ and $g_{\perp} = 2.001 \pm 0.001$), which are indicative of peroxyl radicals (Figure 1).[10] This is consistent with previous observations that all amino-acid-based peroxyl radicals have similar g values at 9 GHz.[31] In Figure 1, the broad $g_{||}$ features for the Trp and His radicals may indicate the presence of two different superimposed signals.

Broadening of the 9 GHz spectra of the protein radicals is primarily due to unresolved proton hyperfine couplings. At higher frequencies, the g anisotropy dominates over the hyperfine interactions. Figure 2a shows that the broadening observed in the 9 GHz spectrum of the Mb radical (top) was significantly reduced at 34 GHz (bottom), providing better resolution of the $g_{\perp}$ region. Figure 2b displays a close-up of the $g_{\perp}$ region of the 34 GHz (Q-band) EPR spectra of the Mb-, Tyr-, Trp-, and His-based radicals. At 34 GHz, the g_Y and g_Z components become better resolved for the Mb and His radicals. The feature resolved at $g = 2.0082$ for the Trp radical could be due to the overlapping g_X component from another radical.

Because the spectral resolution at 9−34 GHz was not adequate for distinguishing between the peroxyl radicals, measurements at 95, 190, and 287 GHz were carried out.

Myoglobin. The HF-EPR spectra of the Mb radical, taken at three different frequencies (Figure 3), were scaled roughly with frequency by plotting the data as a function of g values. The 10 K EPR spectra measured at 96.6, 193.2, and 286.6 GHz exhibit well-resolved g anisotropy with the principal components of a rhombic **g** tensor. At 286.6 GHz, the g_X component is too broad to be observed. The g values of the Mb peroxyl radical were determined from the 287 GHz spectrum using the corrected field axes by calibrating the field with the Mn^{2+} standard. The obtained **g** tensor of the Mb radical ($g_X = 2.035\,60$, $g_Y =$

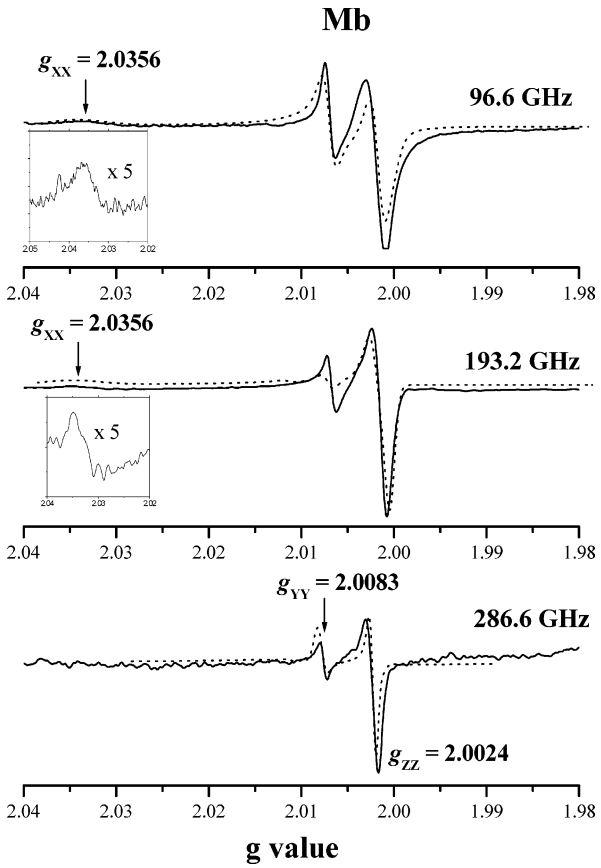

Figure 3. High-field EPR spectra of the Mb radical (10 K) measured at 96.6, 193.2, and 286.6 GHz using a field modulation of 20.9 mA and a frequency modulation of 21.4 kHz. Experimental, solid line; simulated, dotted line.

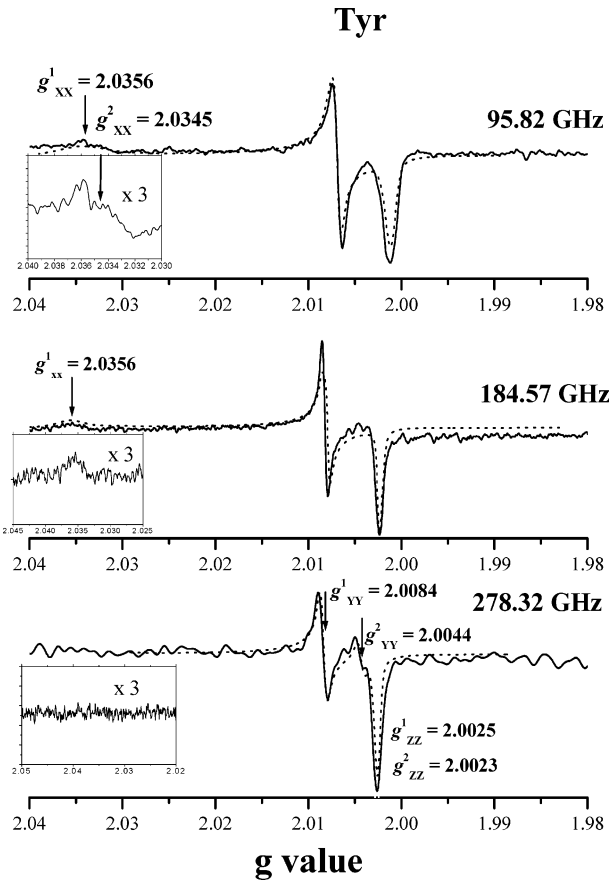

Figure 4. High-field EPR spectra of the Tyr radical (experimental, solid line; simulated, dotted line) measured at 10 K at 95.82, 184.57, and 278.32 GHz using a field modulation of 21.6 mA and a frequency modulation of 21.4 kHz.

2.008 29, and g_Z = 2.002 40) was compared to those of the Tyr, Trp, and His radicals produced by irradiation of the corresponding amino acid/H_2O_2 mixture.

Tyrosine. The HF-EPR spectra of the Tyr peroxyl radical measured at 95.82, 184.57, and 278.32 GHz show the presence of two superimposed signals with rhombic **g** tensors (Figure 4). The principal components of the **g** tensors were determined by spectral simulation. The HF-EPR spectra of the Tyr radical as well as those of the Trp and His radicals can be well-simulated as isolated radicals. Two signals exhibit two resolved g_X components, g^1_X = 2.0356 and g^2_X = 2.0345 at 95.82 GHz. The g_Y and g_Z features of the two radicals are not separated at this frequency. With the frequency increased to 184.57 GHz, the g^2_X component was no longer observable because of line width broadening. Neither g^1_X nor g^2_X features were observed at 278.32 GHz. In contrast, the g_Y features become narrower and better resolved at higher frequencies. The g_Z features of the two radicals were unresolved even at 278 GHz and were obtained from spectral simulations. The two overlapping signals are most likely due to peroxyl radicals formed at two different sites of tyrosine. The initial hydroxyl radical (•OH) formed upon reaction of tyrosine with H_2O_2 can abstract a proton from the phenol and the methylene group (see Chart 2), producing two different Tyr radicals. Subsequent reaction of the radicals with molecular oxygen affords the peroxyl radicals.

Tryptophan. HF-EPR spectra of the Trp peroxyl radical were also taken at three different frequencies (Figure 5). At 95 GHz and higher frequencies, the spectra show overlap of two signals with effective components of the rhombic **g** tensors. The spectra were simulated with reasonable accuracy to obtain the principal components of the **g** tensors (2.037 90, 2.003 75, and 2.001 95

CHART 2

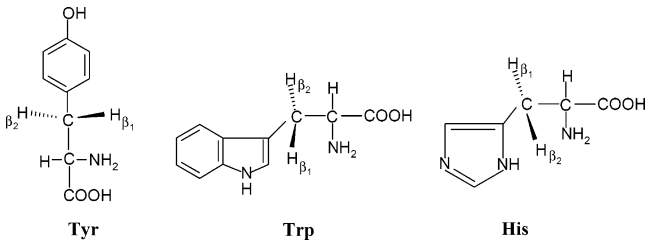

Tyr **Trp** **His**

TABLE 1: *g* Values of the Mb, Tyr, Trp, and His Peroxyl Radicals

peroxyl radicals	g_X	g_Y	g_Z
Mb	2.035 60	2.008 29	2.002 40
Tyr (1)	2.035 60	2.008 40	2.002 50
(2)	2.034 50	2.004 40	2.002 30
Trp (1)	2.037 90	2.003 75	2.001 95
(2)	2.008 22	2.002 95	2.001 80
His (1)	2.060 50	2.007 50	2.000 60
(2)	2.036 30	2.006 90	2.000 40

and 2.008 22, 2.002 95, and 2.001 80). The g^1_X = 2.0379 feature detected at 9−34 GHz was not observed at 95−288 GHz. The g_X feature from the second radical (g^2_X = 2.008 22) is better resolved at 95−190 GHz but at 288 GHz becomes too broad to be observed. The resolution of the g_Y components increases significantly with a frequency increase from 95 to 288 GHz. The g_Z components of two radicals were obtained from the 288 GHz spectrum simulation. The broadening of the g_X components at higher frequencies is indicative of an inhomogeneous environment. Two Trp radical signals separated at 95−288 GHz

TABLE 2: Parameters Used in the Simulation of the 286.6 GHz Mb Spectrum with the $S^{Fe} = 1$, $S^{Rad} = {}^1/_2$ Model

	g_X	g_Y	g_Z
	Radical		
radical g values	2.0356	2.0083	2.0024
Gaussian distribution about g (σ_X and σ_Y)	0.0007	0.0002	
	Oxoferryl Heme		
oxoferryl species g values	2.25	2.25	1.98
zero-field splitting parameters of the Fe	$D = 660$ GHz	$E = 0$	
	Interaction		
dipolar coupling constant	0.170 GHz		
isotropic exchange constant	$J = 0.476$ GHz		
Rad−Fe distance	$R = 8.30$ Å		

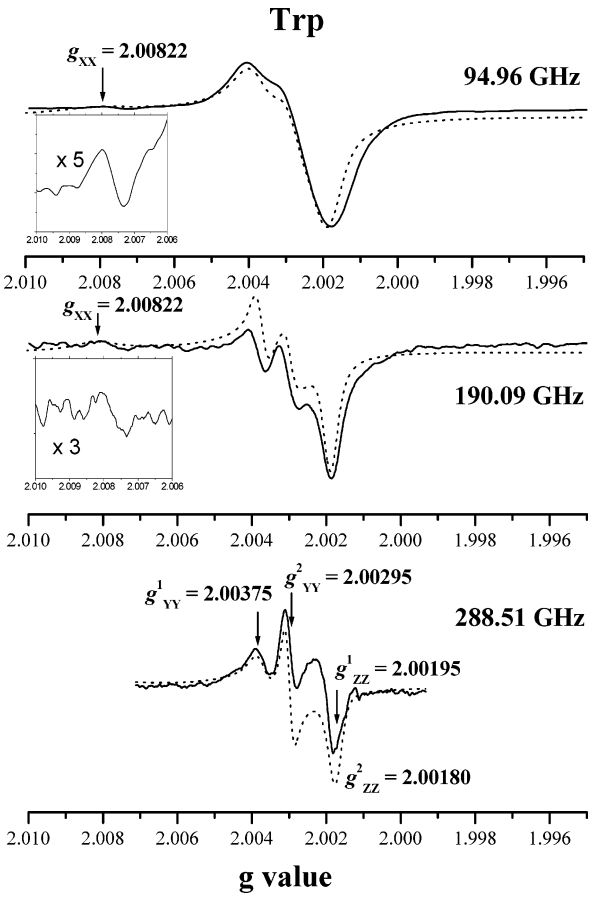

Figure 5. High-field EPR spectra of the Trp radical (experimental, solid line; simulated, dotted line) measured at 10 K at 94.96, 190.09, and 288.51 GHz using a field modulation of 9.65−21 mA and a frequency modulation of 21.4 kHz.

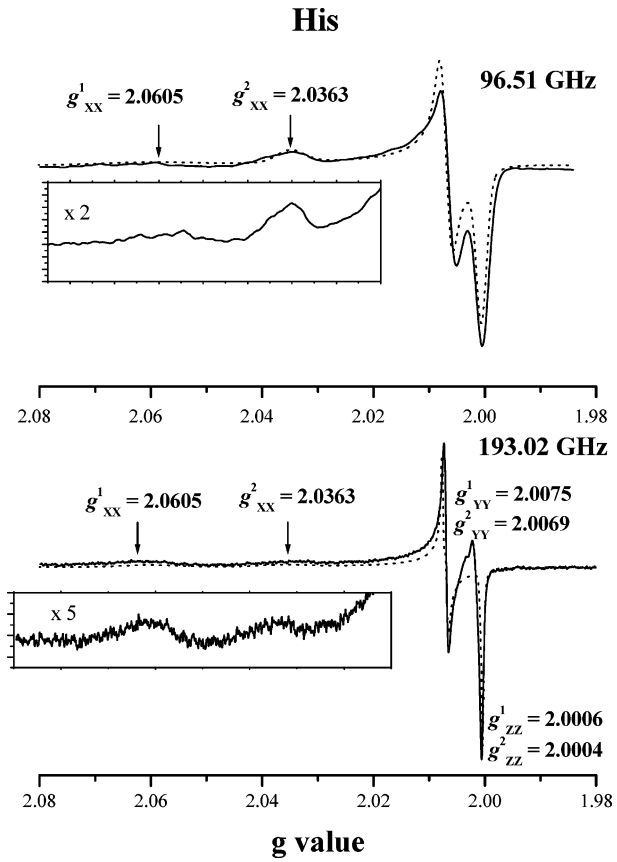

Figure 6. High-field EPR spectra of the His radical (experimental, solid line; simulated, dotted line) measured at 10 K at 96.51 and 193.02 GHz using a field modulation of 16−47 mA and a frequency modulation of 9.5−21.4 kHz.

are attributable to peroxyl radicals formed at two different Trp sites. Irradiation of the Trp amino acid−hydrogen peroxide mixture presumably results in initial formation of the •OH radical which can abstract a hydrogen from the nitrogen of the tryptophan indole ring or the methylene group (Chart 2), producing two different Trp radicals which in turn react with O_2 to form the peroxyl radicals.

Histidine. The HF-EPR spectra of the His radical measured at 96.51 and 193.02 GHz are shown in Figure 6. Again, two different peroxyl radicals can be identified from the spectra. The well-separated g_X components of the rhombic **g** tensor show the same trend as those observed for the Trp and Tyr radicals. These features become broader with increasing frequency. The g_Y and g_Z components were determined from the 193 GHz spectrum simulation. The detected peroxyl radicals are due to two different His radicals produced via hydrogen abstraction from the nitrogen atom of the imidazole ring and the methylene group (Chart 2).

The g values of the peroxyl radicals obtained from the best fits of the simulated and experimental data are summarized in Table 1.

The **g** tensor of the Mb radical estimated from the 287 GHz spectrum is nearly identical with that determined from the simulated high-field EPR spectra of the isolated Tyr peroxyl radical. We assumed that the Tyr residue is the most likely candidate for the peroxyl radical location in Mb. According to the crystal structure, both the Tyr103 and Tyr146 residues are close enough to the heme iron (see Chart 1) and can participate in Mb oxidation. To identify the specific Tyr residue responsible for the radical location in Mb, we have to determine the distance between the radical and the iron of the heme. Therefore, the

HF-EPR powder spectra of the Mb radical were simulated taking into consideration exchange coupling between the protein radical and the oxoferryl heme species. A weak interaction between the oxoferryl species and the animo acid radical has been proposed by Houseman et al.[32,33] The HF-EPR spectra of exchange-coupled oxoferryl−protein radical pairs were previously analyzed for cytochrome *c* peroxidase (CcP)[22] and prostaglandin H-synthase (PGHS).[23] Analysis of spin-coupled systems provides the opportunity to estimate a distance between interacting spins from the dipolar part of the interaction.[34−37]

Spectral Simulations. The total spin Hamiltonian that describes the interacting system of an oxoferryl spin $\mathbf{S} = 1$ ($\mathbf{S}^{Fe}$) with a radical spin $\mathbf{S} = {}^1/_2$ ($\mathbf{S}^{rad}$) is the sum of two Zeeman terms for the isolated centers, zero-field splitting of the oxoferryl heme, represented by the third term, and the interaction term ($\mathbf{S}^{rad}\cdot\Delta\cdot\mathbf{S}^{Fe}$) which accounts for the anisotropic dipole−dipole and the isotropic exchange interaction between a pair of paramagnetic centers:[22,32]

$$\hat{\boldsymbol{H}} = \beta\mathbf{S}^{rad}\cdot\mathbf{g}^{rad}\cdot\boldsymbol{B} + \beta\mathbf{S}^{Fe}\cdot\mathbf{g}^{Fe}\cdot\boldsymbol{B} + \mathbf{S}^{Fe}\cdot\mathbf{D}^{Fe}\cdot\mathbf{S}^{Fe} + \mathbf{S}^{rad}\cdot\Delta\cdot\mathbf{S}^{Fe} \quad (1)$$

where β is the Bohr magneton; $\boldsymbol{B}$ is the applied magnetic field; $\mathbf{g}^{rad}$ and $\mathbf{g}^{Fe}$ are the **g** tensors of the radical and the iron species, respectively; **D** is the zero-field splitting tensor for iron; Δ is the interaction tensor; and $\mathbf{S}^{rad}$ and $\mathbf{S}^{Fe}$ are the vector spin operators. The isotropic component of the tensor Δ is due to Heisenberg exchange coupling (J). The anisotropic component is modeled by an axial dipolar coupling (D):

$$\Delta_{zz} = -J - 2D(\cos^2\theta - {}^1/_3) \quad (2)$$

$$\Delta_{\pm} = -(J + D(\cos^2\theta - {}^1/_3))/2 \quad (3)$$

where θ is the angle between the magnetic field and the axis joining the two point dipoles.

If we assume a point-dipole approximation for the dipole−dipole interaction, with two centers separated by a distance of r, the dipole coupling coefficient (D) is given by eq 4:

$$D = \mu^0 g^{Fe} g^{rad} \beta^2 / 4\pi r^3 \quad (4)$$

The HF-EPR spectra of Mb radical were simulated by using the XSophe computer simulaton software which includes a powder matrix diagonalization approach. The parameters used in the simulation are listed in Table 2. The simulated spectra are shown in Figure 3 (dotted lines) together with the experimental data.

The zero-field splitting tensor of the iron species is assumed to be axial. The estimated parameter $D^{Fe} \sim 660$ GHz[22,38] was fixed in the simulations. The **g** tensor used for the oxoferryl moiety was $g_X = g_Y = 2.25$ and $g_Z = 1.98$.[33,38] These parameters along with the g values obtained for the isolated Tyr radical were used to simulate the dipolar and exchange interactions between two paramagnetic species. Thus, the adjustable parameters in the simulations were D, J, and the angle between the magnetic field direction and the axis joining the two radicals. To reproduce the large width of the g_X peak and the high-field tail of the signal which results from the breadth of the g_Y feature, it was necessary to use a distribution about the values (σ_X and σ_Y), as pointed out by Houseman et al.[32] The g-strain line shape model incorporated into the XSophe program provided an accurate simulation of the line widths of the Gaussian distributions about the g values. A distribution in g_X and g_Y values with Gaussian line widths of 0.0007 and 0.0002, respectively, reproduced the spectral broadening well.

The spin-coupled 287 GHz spectrum of Mb was best fitted with the exchange coupling value (J) 0.476 GHz and the dipole coupling value (D) 0.170 GHz. The dipolar coupling obtained from the simulations yields a spin−spin distance of ∼8.3 Å, which is consistent with the distance from the heme iron to the phenoxyl oxygen of the Tyr146 residue determined from the crystal structure.[28] A comparison with values reported for exchange-coupled systems[22,36] shows that such a distance is compatible with the values found for J and D.

The 96.6−193.2 GHz spectra of the Mb radical were well-simulated by using the parameters determined from the 286.6 GHz spectrum simulation. It should be emphasized that, if interaction parameters are left out from the simulations, the lower frequency 96.6−193.2 GHz spectra cannot be well-fitted by the use of the g values obtained from the 286.6 GHz spectrum.

4. Conclusions

Multifrequency EPR spectroscopy was applied to identify the location of the peroxyl radical in myoglobin oxidized by hydrogen peroxide. The EPR parameters of the radical produced in Mb treated with H_2O_2 were compared with those of the radicals formed by photo-oxidation of the individual amino acids, namely, Tyr, Trp, and His. The EPR spectra of the peroxyl radicals have similar g values at X-band frequency (9 GHz). In contrast, at higher frequencies (95−287 GHz), it is possible to resolve the g anisotropy of amino-acid-based radicals and to distinguish between them. Taking into account that the **g** tensor determined from the 287 GHz spectrum of the Mb radical is similar to that obtained for the isolated Tyr radical, we conclude that the tyrosine residue is a good candidate for the peroxyl radical location in myoglobin.

The simulations of the exchange-coupled Mb spectra yield a spin−spin distance of 8.3 Å, which is consistent with the distance between the iron of the heme and the tyrosine residue at position 146. In the approach we used, the dipolar interaction term has axial symmetry and we assumed the point-dipole approximation.

Multifrequency HF-EPR spectroscopy is a promising tool for investigating the heme-protein oxidation by hydroperoxides. This technique increases the g value resolution and facilitates analysis of the protein radicals observed as powder patterns or existing as exchange-coupled systems between a protein radical and the oxoferryl moiety.

Acknowledgment. This work was supported by the Division of Chemical Sciences, Office of Basic Energy Sciences, Office of Energy Research, the U.S. Department of Energy, Grant DE-FG02-86ER13465, and the NSF supported National High Magnetic Field Laboratory (Tallahassee, Florida).

References and Notes

(1) Grisham, M. B.; Everse, J. *Peroxidases in Chemistry and Biology*; Everse, J., Everse, K. E., Grisham, M. B., Eds.; CRC Press Inc.: Boca Raton, FL, 1991; Vol. 1, pp 335−344.

(2) Stadtman, E. R. *Biochemistry* **1990**, *29*, 6323−6331.

(3) Mieyal, J. J. *Reviews in Biochemical Technology*; Hodgson, E., Bend, J. R., Philpot, R. M., Eds.; Elsevier: New York, 1985; Vol. 7, pp 1−66.

(4) Dunford, H. B. *Peroxidases in Chemistry and Biology*; Everse, J., Everse, K. E., Grisham, M. B., Eds.; CRC Press Inc.: Boca Raton, FL, 1991; Vol. 2, pp 1−24.

(5) Harada, K.; Yamazaki, I. *J. Biochem. (Tokyo)* **1987**, *101*, 283−286.

(6) King, N. K.; Winfield, M. E. *J. Biol. Chem.* **1963**, *238*, 1520−1528.

(7) Gibson, J. F.; Ingram, D. J. E.; Nicholls, P. *Nature* **1985**, *181*, 1398−1399.
(8) King, N. K.; Looney, F. D.; Winfield, M. E. *Biochim. Biophys. Acta* **1967**, *133*, 65−82.
(9) Gunther, M. R.; Tschirret-Guth, R.; Witkowska, H. E.; Fann, Y. C.; Barr, D. P.; Ortiz de Montellano, P. R.; Mason, R. P. *Biochem. J.* **1998**, *330*, 1293−1299.
(10) Kelman, D. J.; DeGray, J. A.; Mason, R. P. *J. Biol. Chem*. **1994**, *269*, 7458−7463.
(11) King, N. K.; Looney, F. D.; Winfield, M. E. *Biochim. Biophys. Acta* **1967**, *133*, 65−82.
(12) Rao, S. I.; Wilks, A.; Ortiz de Montellano, P. R. *J. Biol. Chem*. **1993**, *268*, 803−809.
(13) Davies, M. J. *Free Radical Res. Commun.* **1990**, *10*, 361−370.
(14) Arduini, A.; Mancinelli, G.; Radatti, G. L.; Damonti, W.; Hochstein, P.; Cadenas, E. *Free Radical Biol. Med*. **1992**, *13*, 449−454.
(15) Wilks, A.; Ortiz de Montellano, P. R. *J. Biol. Chem*. **1992**, *267*, 8827−8833.
(16) DeGray, J. A.; Gunther, M. R.; Tschirret-Guth, R.; Ortiz de Montellano, P. R.; Mason, R. P. *J. Biol. Chem*. **1997**, *272*, 2359−2362.
(17) Gunther, M. R.; Kelman, D. J.; Corbett, R. P.; Mason, R. P. *J. Biol. Chem*. **1995**, *270*, 16075−16081.
(18) Witting, P. K.; Douglas, D. J.; Grant Mauk, A. *J. Biol. Chem*. **2000**, *275*, 20391−20398.
(19) Fenwick, C. W.; English, A. M. *J. Am. Chem. Soc*. **1996**, *118*, 12236−12237.
(20) Gerfen, G. J.; Bellew, B. F.; Un, S.; Bollinger, J. M.; Stubbe, J.; Griffin, R. G.; Singel, D. J. *J. Am. Chem. Soc*. **1993**, *115*, 6420−6421.
(21) Prisner, T. F.; McDermott, A. E.; Un, S.; Norris, J. R.; Thurnauer, M. C.; Griffin, R. G. *Proc. Natl. Acad. Sci. U.S.A.* **1993**, *90*, 9485−9488.
(22) Ivancich, A.; Dorlet, P.; Goodin, D. B.; Un, S. *J. Am. Chem. Soc*. **2001**, *123*, 5050−5058.
(23) Dorlet, P.; Seibold, S. A.; Babcock, G. T.; Gerfen, G. J.; Smith, W. L.; Tsai, A.; Un, S. *Biochemistry* **2002**, *41*, 6107−6114.
(24) Dorlet, P.; Boussas, A.; Rutherford, W.; Un, S. *J. Phys. Chem. B* **1999**, *103*, 10945−10954.
(25) Bar, G.; Bennati, M.; Nguyen, H.-H. T.; Ge, J.; Stubbe, J. Griffin, R. G. *J. Am. Chem. Soc*. **2001**, *123*, 3569−3576.
(26) Un, S.; Atta, M.; Fontecave, M.; Rutherford, W. A. *J. Am. Chem. Soc*. **1995**, *117*, 10713−10719.
(27) Ivancich, A.; Mattioli, T. A.; Un, S. *J. Am. Chem. Soc*. **1999**, *121*, 5743−5753.
(28) Maurus, R.; Overall, C. M.; Bogumil, R.; Luo, Y.; Mauk, A. G.; Smith, M.; Brayer, G. D. *Biochim. Biophys. Acta* **1997**, *1341*, 1.
(29) Catalano, C. E.; Choe, Y. S.; Ortiz de Montellano, P. R. *J. Biol. Chem*. **1989**, *264*, 10534−10541.
(30) Mueller, F.; Hopkins, M. A.; Coron, N.; Grynberg, M.; Brunel, L. C.; Martinez, G. *Rev. Sci. Instrum.* **1989**, *60*, 3681.
(31) Dimmey, L. J.; Gordy, W. *Proc. Natl. Acad. Sci. U.S.A.* **1980**, *77*, 343−346.
(32) Houseman, A. L.; Doan, P.; Goodin, D. B.; Hoffman, B. M. *Biochemistry* **1993**, *32*, 4430−4443.
(33) Huyett, J. E.; Doan, P. E.; Gurblel, R.; Houseman, A. L. P.; Sivaraja, M.; Goodin, D. B.; Hoffman, B. M. *J. Am. Chem. Soc*. **1995**, *117*, 9033−9041.
(34) Lakshmi, K. V.; Eaton, S. S.; Eaton, G. R.; Frank, H. A.; Brudvig, G. W. *J. Phys. Chem. B* **1998**, *102*, 8327−8335.
(35) Peloquin, J. M.; Campbell, K. A.; Britt, R. D. *J. Am. Chem. Soc*. **1998**, *120*, 6840−6841.
(36) Dorlet, P.; Valentin, M. D.; Babcock, G. T.; McCracken, J. L. *J. Phys. Chem. B* **1998**, *102*, 8239−8247.
(37) Force, D. A.; Randall, D. W.; Britt, R. D. *Biochemistry* **1997**, *36*, 12062−12070.
(38) Schulz, C. E.; Devaney, P. W.; Wrinkler, H.; Debrunner, P. G.; Doan, N.; Chiang, R.; Rutter, R.; Hager, L. P. *FEBS Lett*. **1979**, *103*, 102−105.